

Automatic ictal HFO detection for determination of initial seizure spread

Andreas Graef, Christoph Flamm, Susanne Pirker, Christoph Baumgartner,
Manfred Deistler, *Fellow, IEEE*, and Gerald Matz, *Senior Member, IEEE*

Abstract—High-frequency oscillations (HFOs) are a reliable indicator for the epileptic seizure onset zone (SOZ) in ECoG recordings. We propose a novel method for the automatic detection of ictal HFOs in the ripple band (80-250Hz) based on CFAR matched sub-space filtering. This allows to track the early propagation of ictal HFOs, revealing initial and follow-up epileptic activity on the electrodes. We apply this methodology to two seizures from one patient suffering from focal epilepsy. The electrodes identified are in very good accordance with the visual HFO analysis by clinicians. Furthermore the electrodes with initial HFO activity are correlated well with the SOZ (conventional ϑ -activity).

I. INTRODUCTION

A. Background

Epilepsies, defined as disorders with recurrent unprovoked seizures, affect approximately 0.7% of the general population [1]. Seizures are characterized by abnormal synchronized neuronal discharge of networks in both hemispheres (generalized seizures) or in circumscribed networks in one hemisphere (focal seizures). About one third of focal epilepsy patients suffer from drug resistance, and epilepsy surgery has become a valuable treatment option for them [2]. If a clear-cut definition of the seizure onset zone is possible, the goal is the removal of the epileptogenic tissue in order to abolish the seizures [3]. Up to 70% of patients with drug resistant focal epilepsy become seizure free following surgery [4]. Presurgical evaluation comprises prolonged video-EEG recording, high resolution brain imaging as well as neuropsychological tests. If scalp EEG cannot provide sufficient information on the seizure onset zone (SOZ), invasive recording using subdural strip electrodes (*electrocorticography, ECoG*), which are placed directly on the cortex, is performed in order to determine the epileptic focus [5].

Clinical experts perform the analysis of initial seizure propagation including the determination of the SOZ by visual inspection of the raw ECoG recordings. This current gold standard (cf. [6] and [7] for two recent studies) is based

on the onset of ictal rhythmic activity (mostly in the ϑ - or δ -frequency band, [8]). In the last years, a new class of biomarkers has received growing attention [9]: *high-frequency oscillations (HFOs)*, which are low-amplitude EEG correlates commonly observed in two sub-bands, as ripples (80-250Hz) and fast ripples (250-500Hz). They occur interictally as well as ictally [10], and interictal HFOs are excellent markers of the SOZ (higher sensitivity and specificity than spikes, cf. e.g. [11], [12]). In the following we will be interested in ictal HFOs only. They correlate well with the SOZ as well (cf. e.g. [13]) and typically occur several seconds before conventional EEG onset, with a range between 8s [14] and 20s [15].

B. Contributions and state of the art

The visual inspection of ECoG data for HFO analysis is a time-demanding, highly subjective task which depends heavily on the individual experience of the investigator. Therefore we suggest a complementary computational approach based on classical signal detection methodology, compare subsection II-A.

Several automated HFO detection algorithms have already been proposed in literature. First attempts included rather simple approaches based on band-pass filtering and subsequent use of detection statistics like RMS [16], Teager Energy [17], Line Length ([18] and [19]) or the Hilbert transform [20].

In order to decrease false-positives, increasingly complicated multi-step approaches based on the above ideas have come up in the last years, e.g. [21], [22] and [23], and very recently [24].

While these studies focus on the automatic detection of HFOs in interictal EEG (or in databases including ictal and interictal phases), we limit ourselves to the analysis of ictal ECoG recordings. In contrast to the aforementioned approaches, we are not interested in the generation of statistics of HFO rates, but want to track the spread of initial HFOs. For this analysis, seizure onset time is provided by clinicians.

Therefore, our contributions to the area of HFO analysis are twofold:

- 1) We propose a novel algorithm for automatic detection of HFOs.
- 2) We track the propagation of initial ictal HFOs. Channels showing first HFOs indicate the SOZ (of conventional ictal activity).

Manuscript received April 12th, 2013

A. Graef (e-mail: andreas.graef@tuwien.ac.at), C. Flamm and M. Deistler are with Vienna University of Technology, Institute for Mathematical Methods in Economics; Vienna, Austria.

G. Matz is with Vienna University of Technology, Institute of Telecommunications; Vienna, Austria

S. Pirker and C. Baumgartner are with Hospital Hietzing with Neurological Center Rosenhügel; Vienna, Austria.

II. METHOD AND MATERIALS

In our analysis we consider multivariate signals consisting of K channels $y_k[n]$, $k = 1, \dots, K$, where n denotes the time index.

A. HFO detection

In order to detect the HFOs in the ripple band, we employ classical methods of signal detection, namely an implementation of the CFAR (constant false alarm rate) matched subspace filter according to [25]. The main idea of this detector is to compare the power of the signal content in the ripple band to the power of the residual signal. For this purpose we proceed as follows for each channel k :

- We initially perform a pre-emphasis step: We apply a high-pass filter at 13Hz (upper bound of the α -band) to the signal $y_k[n]$ in order to compensate for the strong spectral roll-off of ECoG data. We denote the spectrally equalized signal by $x_k[n]$.
- Second, we apply a band-pass filter in the frequency range of 75-250Hz to obtain $x_k^R[n]$.
- In a next step we calculate the power ratio for the CFAR matched sub-space filter. We calculate the statistic as

$$T^2[n] = \frac{|\mathcal{H}\{x_k^R\}[n]|^2}{|\mathcal{H}\{x_k - x_k^R\}[n]|^2},$$

where $\mathcal{H}\{x\}[n]$ denotes the (complex-valued) Hilbert transform of x at time-point n . As is well known [26], the envelope of x , $|\mathcal{H}\{x\}[n]|^2$, indicates the (instantaneous) power of the signal. Thus the numerator represents the power in the ripple band, the denominator the power of the residual signal.

- We detect the presence of HFOs if $T[n] > \gamma$. The threshold γ is determined from a reference period prior to the ictal activity. In order to suppress false-positives due to sharp transients, we demand $T[n] > \gamma$ continuously for at least 50ms (corresponding to 4 cycles of an 80Hz oscillation).

B. ECoG data

The ECoG data used in this study are taken from a patient (male, 43 years) suffering from therapy-resistant focal epilepsy. The patient underwent a presurgical long-term video EEG monitoring at the Hospital Hietzing with Neurological Center Rosenhügel. Three subdural strip electrodes with a total of 25 channels were implanted, and the electrode B1 (outside the seizure focus) was chosen as reference. Compare the MRI (magnetic resonance imaging) scan in Fig. 3 for details.

Recording was performed using a Micromed[®] system at a sampling frequency of 1024Hz. Four seizures occurred within 2 hours during the monitoring period, but initial ictal HFOs in the ripple band are only present in the first two. Note that a visual inspection did not reveal any fast ripples, thus this study is limited to the ripple band.

After recording, the ECoG data were preprocessed in Matlab[®]: Line interference and its super-harmonics were

removed using notch filters at 50 Hz, 150Hz, 250Hz and 350Hz. The signals were low-pass filtered at 256 Hz in order to avoid aliasing and then downsampled to 512 Hz.

C. Test signal

In order to demonstrate the effectiveness of the proposed algorithm, we test it on simulated data in subsection III-A.

For this purpose we fit an AR-8 model to channel A12 in a 20-second lasting period 30 seconds prior to seizure 1. Based on these parameter estimates, we simulate 5 seconds of an AR-8 signal $s[n]$. The test signal then contains superposed HFOs during 0.5 seconds, i.e.

$$y[n] = \begin{cases} s[n] & n = 1 \dots 2f_s, \\ s[n] + a \sin\left(\frac{2\pi n f}{f_s}\right) & n = 2f_s + 1 \dots 2.5f_s, \\ s[n] & n = 2.5f_s + 1 \dots 5f_s. \end{cases}$$

The variance of the white noise in the AR simulation step was set to $\sigma^2 = 5$, which resulted in a HFO-to-background SNR of -2.7dB.

In order to facilitate the comparison with ECoG data, a sampling frequency f_s of 512Hz is used for simulation. We set the frequency to $f = 85$ and the amplitude to $a = 12$ to obtain simulated ripples, compare plot (a) of Fig. 1.

III. RESULTS

A. Simulation

In order to assess our methodology, we apply the HFO detection algorithm to the test signal described in subsection II-C. The threshold γ is calculated as the 90%-percentile of $T[n]$ from $s[n]$.

Fig. 1 details the results: The simulated HFOs are correctly detected in the time interval 2.0s - 2.5s, see the HFO detection sequence in plot (d). During this period the statistic $T[n]$ takes large values, see plot (c). Sporadic short threshold exceedings of $T[n]$ are successfully suppressed.

Note that for better visualization a spectrogram is shown in plot (b). It clearly reveals the presence of the simulated HFOs.

B. Onset zone analysis

We apply the proposed methodology to the first two seizures. In each case, the threshold γ was determined as the 90%-percentile of the statistic $T[n]$ from a 120-second reference period starting three minutes prior to the respective seizure. Three clinical experts independently analyzed the two seizures by visual inspection and marked the first occurrence of HFOs on each channel. We distinguish between initial, close follow-up (within 250ms) and later HFO activity Table I summarizes the findings of our algorithm and the visual inspection for initial and follow-up activity.

In Fig. 2 we show the results for seizure 1. Detected HFOs are highlighted in red. According to the algorithm, initial HFOs are found on channels B8 and B7. A quick propagation (~ 0.125 s) takes place to channels A11 and A5. Subsequent HFOs are detected on electrodes A and C.

In seizure 2 our algorithm detects initial HFOs on channel A9.

TABLE I
RESULTS OF THE HFO DETECTION ALGORITHM AND COMPARISON TO VISUAL INSPECTION OF HFO- AND CONVENTIONAL ϑ ACTIVITY.

Seizure	Examiner	Initial HFOs initial	HFOs follow-up	Conventional theta activity initial	Conventional theta activity follow-up
1	Algorithm	B8, B7	A11, A5	-	-
	Expert 1	B8, B7	A11, A5, A6, A7, A12	B8	A10, A11, A12
	Expert 2	B8, B7	A11, A5, A6, A7, A12	A11, A12, B8	A9, A10, B7
	Expert 3	B8, B7	A5, A7, A11	A10, A11, A12	B8
2	Algorithm	A9	-	-	-
	Expert 1	A9	C3	A11, A12	A9, A10
	Expert 2	A9	C3, C2	A11, A12	A10
	Expert 3	A9	C3	A11, A12	B8

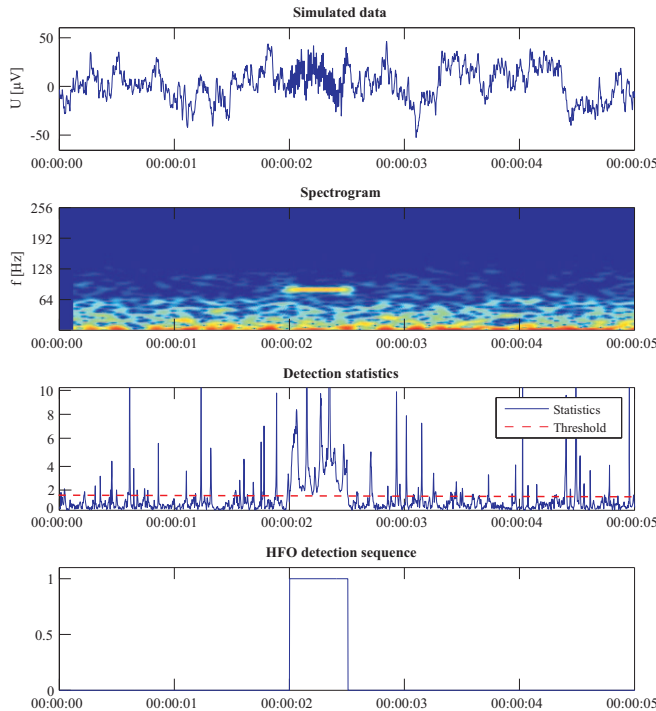


Fig. 1. Simulation results. (a) Simulated test signal, (b) spectrogram, (c) statistic $T[n]$ and threshold γ , (d) HFO detection sequence.

IV. DISCUSSION

In Subsection III-A we showed that our proposed methodology is capable of detecting HFOs in simulated data while suppressing sporadic false alarms. The application of this methodology to invasive EEG recordings (Subsection III-B) yields promising results as well.

In both seizures our method correctly identifies the electrodes with initial HFO activity, B7 and B8 in seizure 1, A9 in seizure 2 (see Table I). These findings match the visual analysis of all three experts.

In case of follow-up HFO activity, our algorithm also yields good results: In seizure 1 we successfully mark close HFO follow-up activity on electrodes A11 and A5. Later HFO activity on other electrodes (A7, A9, C2, C3) is correctly identified, but detection is delayed up to 250ms, compare Fig. 2. In seizure 2 the experts flag electrodes C2 and C3 as follow-

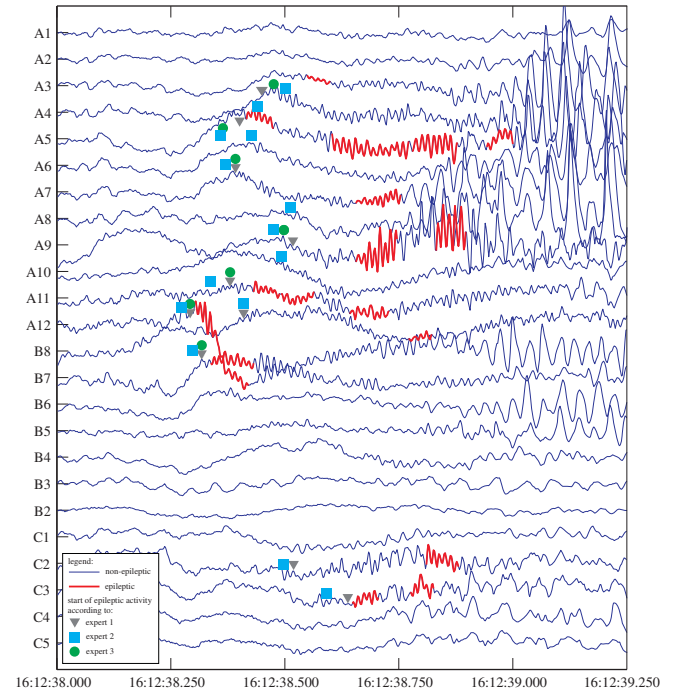


Fig. 2. HFO propagation in seizure 1. Automatically detected HFO activity is highlighted in red. Onset of HFO activity according to the visual analysis of three clinical experts is indicated.

up, whereas our algorithm marks late HFO propagation on C3 with a latency of 500ms (seizure 2 not shown).

The area of initial HFO activity (B7, B8 and A9) correlates well with the SOZ determined by visual inspection of conventional ϑ -activity, compare Table I. Note that the time interval between the occurrence of ictal HFOs and the onset of conventional ϑ -activity is 7s (seizure 1) and 8s (seizure 2), which is in good accordance with literature as mentioned in Subsection I-A.

Based on the results of our HFO analysis we infer that the SOZ comprises the parieto-occipital area between electrodes B7 and A9, see Fig. 3.

V. CONCLUSION

In this paper we proposed a novel method for the detection of HFOs in the ripple band. This pilot study shows promising

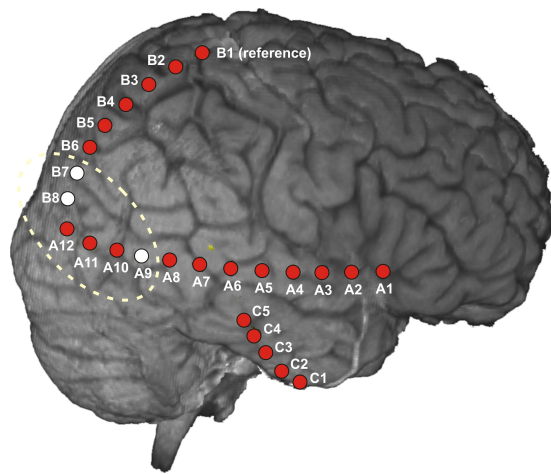


Fig. 3. MRI scan with electrode positions. Electrodes revealing initial ictal HFO activity are marked in white (seizure 1: B7, B8; seizure 2: A9). The supposed seizure onset zone is outlined.

first results in tracking of ictal HFO propagation as an indicator for the SOZ. Therefore we are confident that our method has the potential for an objectivation in the presurgical clinical examination of therapy-resistant patients.

Next necessary steps include the application to a broader data basis and a subsequent statistical analysis (e.g. detection rate/false positives, mean latency in detection) for better understanding of the performance of our method.

ACKNOWLEDGMENTS

This study was supported by the Austrian Science Fund FWF (grant P22961).

We wish to thank Prof. Czech from the Vienna General Hospital, University Clinic for Neurosurgery, for providing the MR image with the subdural electrode strip positions. We are grateful to Sandra Zeckl and Johannes Koren from Neurological Center Rosenhügel for visual inspection of the ECoG recordings.

REFERENCES

- [1] D. Hirtz, D. Thurman, K. Gwinn-Hardy, M. Mohamed, A. Chaudhuri, and R. Zalutsky, "How common are the "common" neurologic disorders?" *Neurology*, vol. 68, pp. 326–337, 2007.
- [2] J. Engel, "Surgery for seizures," *New England Journal of Medicine*, vol. 334, pp. 647–652, 1996.
- [3] S. Schuele and H. Lüders, "Intractable epilepsy: management and therapeutic alternatives," *The Lancet Neurology*, vol. 7, no. 6, pp. 514–524, 2008.
- [4] J. Téllez-Zenteno, R. Dhar, and S. Wiebe, "Long-term seizure outcomes following epilepsy surgery: a systematic review and meta-analysis," *Brain*, vol. 128, pp. 1188–1198, 2005.
- [5] M. Pondal-Sordo, D. Diosy, J. F. Téllez-Zenteno, R. Sahjapaul, and S. Wiebe, "Usefulness of intracranial EEG in the decision process for epilepsy surgery," *Epilepsy Research*, vol. 74, pp. 176–182, 2007.
- [6] K. Götz-Trabert, C. Hauck, K. Wagner, S. Fauser, and A. Schulze-Bonhage, "Spread of ictal activity in focal epilepsy," *Epilepsia*, vol. 49, no. 9, pp. 1594–1601, 2008.
- [7] S. Jenssen, C. Roberts, E. Gracely, D. Dlugos, and M. Sperling, "Focal seizure propagation in the intracranial EEG," *Epilepsy Research*, vol. 93, pp. 25–32, 2011.

- [8] N. Foldvary, G. Klem, J. Hammel, W. Bingaman, I. Najm, and H. Lüders, "The localizing value of ictal EEG in focal epilepsy," *Neurology*, vol. 57, pp. 2022–2028, 2001.
- [9] J. Jacobs, R. Staba, E. Asano, H. Otsubo, J. Y. Wu, M. Zijlmans, I. Mohamed, P. Kahane, F. Dubeau, V. Navarro, and J. Gotman, "High-frequency oscillations (HFOs) in clinical epilepsy," *Progress in Neurobiology*, vol. 98, no. 3, pp. 302–315, 2012.
- [10] M. Zijlmans, J. Jacobs, Y. Kahn, R. Zelman, and F. Dubeau, "Ictal and interictal high frequency oscillations in patients with focal epilepsy," *Clinical Neurophysiology*, vol. 122, pp. 664–671, 2011.
- [11] J. Jacobs, P. LeVan, R. Chander, J. Hall, F. Dubeau, and J. Gotman, "Interictal high-frequency oscillations (80–500 Hz) are an indicator of seizure onset areas independent of spikes in the human epileptic brain," *Epilepsia*, vol. 49, no. 11, pp. 1893–1907, 2008.
- [12] J. Jacobs, R. Zelman, J. Jirsch, R. Chander, C.-E. Chatillon, F. Dubeau, and J. Gotman, "High frequency oscillations (80–500 Hz) in the preictal period in patients with focal seizures," *Epilepsia*, vol. 50, no. 7, pp. 1780–1792, 2009.
- [13] N. Usui, K. Terada, K. Baba, K. Matsuda, F. Nakamura, K. Usui, M. Yamaguchi, T. Tottori, S. Umeoka, S. Fujitani, A. Kondo, T. Mihara, and Y. Inoue, "Clinical significance of ictal high frequency oscillations in medial temporal lobe epilepsy," *Clinical Neurophysiology*, vol. 122, pp. 1693–1700, 2011.
- [14] H. Khosravani, N. Mehrotra, M. Rigby, W. Hader, C. R. Pinnegar, N. Pillay, S. Wiebe, and P. Federico, "Spatial localization and time-dependent changes of electrographic high frequency oscillations in human temporal lobe epilepsy," *Epilepsia*, vol. 50, no. 4, pp. 605–616, 2009.
- [15] H. Imamura, R. Matsumoto, M. Inouchi, M. Matsushashi, N. Mikuni, R. Takahashi, and A. Ikeda, "Ictal wideband ECoG: Direct comparison between ictal slow shifts and high frequency oscillations," *Clinical Neurophysiology*, vol. 122, pp. 1500–1504, 2011.
- [16] R. Staba, C. Wilson, A. Bragin, I. Fried, and J. Engel, "Quantitative Analysis of High-Frequency Oscillations (80–500 Hz) Recorded in Human Epileptic Hippocampus and Entorhinal Cortex," *Journal of Neurophysiology*, vol. 88, pp. 1743–1752, 2002.
- [17] O. Smart, G. Worrell, G. Vachtsevanos, and B. Litt, "Automatic Detection of High Frequency Epileptiform Oscillations from Intracranial EEG Recordings of Patients with Neocortical Epilepsy," *Proceedings of the IEEE Region 5 and IEEE Denver Section Technical, Professional and Student Development Workshop*, pp. 53–58, 2005.
- [18] A. Gardner, G. Worrell, E. Marsh, D. Dlugos, and B. Litt, "Human and automated detection of high-frequency oscillations in clinical intracranial EEG recordings," *Clinical Neurophysiology*, vol. 118, pp. 1134–1143, 2007.
- [19] G. Worrell, A. Gardner, S. Stead, S. Hu, S. Goerss, G. Cascino, F. Meyer, R. Marsh, and B. Litt, "High-frequency oscillations in human temporal lobe: simultaneous microwire and clinical macroelectrode recordings," *Brain*, vol. 131, pp. 928–937, 2008.
- [20] B. Crépon, V. Navarro, D. Hasboun, S. Clemenceau, J. Martinerie, M. Baulac, C. Adam, and M. Le Van Quyen, "Mapping interictal oscillations greater than 200 Hz recorded with intracranial macroelectrodes in human epilepsy," *Brain*, vol. 133, pp. 33–45, 2010.
- [21] R. Zelman, F. Mari, J. Jacobs, M. Zijlmans, F. Dubeau, and J. Gotman, "A comparison between detectors of high frequency oscillations," *Clinical Neurophysiology*, vol. 123, pp. 106–116, 2012.
- [22] J. Blanco, M. Stead, A. Krieger, J. Viventi, W. R. Marsh, K. Lee, G. Worrell, and B. Litt, "Unsupervised Classification of High-Frequency Oscillations in Human Neocortical Epilepsy and Control Patients," *Journal of Neurophysiology*, vol. 104, pp. 2900–2912, 2010.
- [23] J. Blanco, M. Stead, A. Krieger, W. Stacey, D. Maus, E. Marsh, J. Viventi, K. Lee, R. Marsh, B. Litt, and G. Worrell, "Data mining neocortical high-frequency oscillations in epilepsy and controls," *Brain*, vol. 134, pp. 2948–2959, 2011.
- [24] N. von Ellenrieder, L. Andrade-Valenca, F. Dubeau, and J. Gotman, "Automatic detection of fast oscillations (40–200 Hz) in scalp EEG recordings," *Clinical Neurophysiology*, vol. 123, pp. 670–680, 2012.
- [25] L. L. Scharf, *Statistical Signal Processing*. Addison-Wesley, 1991.
- [26] J. Ville, "Théorie et application de la notion de signal analytique," *Cables et transmission*, vol. 2, no. 1, pp. 61–74, 1948.